



**HAL**  
open science

# Phylogenetic comparative approach reveals evolutionary conservatism, ancestral composition, and integration of vertebrate gut microbiota

Benoît Perez-Lamarque, Guilhem Sommeria-Klein, Loréna Duret, Hélène Morlon

## ► To cite this version:

Benoît Perez-Lamarque, Guilhem Sommeria-Klein, Loréna Duret, Hélène Morlon. Phylogenetic comparative approach reveals evolutionary conservatism, ancestral composition, and integration of vertebrate gut microbiota. *Molecular Biology and Evolution*, 2023, 10.1093/molbev/msad144 . hal-04133633

**HAL Id: hal-04133633**

<https://hal.sorbonne-universite.fr/hal-04133633v1>

Submitted on 20 Jun 2023

**HAL** is a multi-disciplinary open access archive for the deposit and dissemination of scientific research documents, whether they are published or not. The documents may come from teaching and research institutions in France or abroad, or from public or private research centers.

L'archive ouverte pluridisciplinaire **HAL**, est destinée au dépôt et à la diffusion de documents scientifiques de niveau recherche, publiés ou non, émanant des établissements d'enseignement et de recherche français ou étrangers, des laboratoires publics ou privés.



Distributed under a Creative Commons Attribution 4.0 International License

1           **Phylogenetic comparative approach reveals evolutionary**  
2           **conservatism, ancestral composition, and integration of vertebrate**  
3           **gut microbiota**

4  
5  
6           Benoît Perez-Lamarque <sup>1,2\*</sup> (ORCID: 0000-0001-7112-7197)

7           Guilhem Sommeria-Klein <sup>3</sup> (ORCID: 0000-0002-5331-3639)

8           Loréna Duret <sup>1</sup> (ORCID: 0000-0001-7031-4900)

9           Hélène Morlon <sup>1</sup> (ORCID: 0000-0002-3195-7521)

10  
11  
12       <sup>1</sup> *Institut de biologie de l'École normale supérieure (IBENS), École normale supérieure,*  
13       *CNRS, INSERM, Université PSL, 46 rue d'Ulm, 75 005 Paris, France*

14  
15       <sup>2</sup> *Institut de Systématique, Évolution, Biodiversité (ISYEB), Muséum national d'histoire*  
16       *naturelle, CNRS, Sorbonne Université, EPHE, UA, CP39, 57 rue Cuvier 75 005 Paris,*  
17       *France*

18  
19       <sup>3</sup> *Department of Computing, University of Turku, Yliopistonmäki, 20014 Turku, Finland*

20  
21       \*Correspondence: Benoît Perez-Lamarque (benoit.perez@ens.psl.eu)

22 **Abstract:**

23

24 How host-associated microbial communities evolve as their hosts diversify remains  
25 equivocal: How conserved is their composition? What was the composition of ancestral  
26 microbiota? Do microbial taxa covary in abundance over millions of years? Multivariate  
27 phylogenetic models of trait evolution are key to answering similar questions for  
28 complex host phenotypes, yet they are not directly applicable to relative abundances,  
29 which usually characterize microbiota. Here, we extend these models in this context,  
30 thereby providing a powerful approach for estimating phylosymbiosis (the extent to  
31 which closely related host species harbor similar microbiota), ancestral microbiota  
32 composition, and integration (evolutionary covariations in bacterial abundances). We  
33 apply our model to the gut microbiota of mammals and birds. We find significant  
34 phylosymbiosis that is not entirely explained by diet and geographic location, indicating  
35 that other evolutionary-conserved traits shape microbiota composition. We identify  
36 main shifts in microbiota composition during the evolution of the two groups and infer  
37 an ancestral mammalian microbiota consistent with an insectivorous diet. We also find  
38 remarkably consistent evolutionary covariations among bacterial orders in mammals  
39 and birds. Surprisingly, despite the substantial variability of present-day gut microbiota,  
40 some aspects of their composition are conserved over millions of years of host  
41 evolutionary history.

42

43

44 **Keywords:**

45

46 gut microbiome, interactome, phylosymbiosis, holobiont evolution, phylogenetic signal,  
47 comparative methods.

## 48 **Introduction:**

49

50 Host-associated microbial communities, referred to as the *microbiota*, often play  
51 central roles in the biology of the hosts and their interactions with the environment. As  
52 host clades diversify, the microbiota can furthermore play a key role in the adaptation  
53 of their hosts to different ecological conditions. This raises important questions on the  
54 evolution of the microbiota as hosts diversify. First, how much is microbiota  
55 composition conserved over host evolutionary timescales? While the microbiota can  
56 be quite labile within and between host species (Ley et al. 2008; David et al. 2014;  
57 Hacquard et al. 2015; Hird et al. 2015; Amato et al. 2019), more closely related host  
58 species often tend to have more similar microbiota, a pattern referred to as  
59 *phylosymbiosis* (Brooks et al. 2016; Lim and Bordenstein 2020). In animals, levels of  
60 phylosymbiosis appear to be heterogeneous across tissues (e.g. gut or skin  
61 microbiota) and lineages (Mazel et al. 2018; Lim and Bordenstein 2020; Song et al.  
62 2020; Perez-Lamarque, Krehenwinkel, et al. 2022).

63

64 The presence of a phylogenetic signal in microbiota composition across hosts  
65 could potentially be used to reconstruct ancestral microbiota composition. Ancestral  
66 reconstructions could be particularly useful to detect events during host diversification  
67 associated with major shifts in microbiota composition or to verify hypotheses on  
68 ancestral diets. A phylogenetic signal in microbiota composition may also inform on  
69 potential long-term evolutionary covariations in abundances between microbial taxa.  
70 Positive or negative covariations may arise from direct interactions between microbial  
71 taxa, such as cross-feeding, trophic relationships, or competition (Faust et al. 2012;  
72 Foster et al. 2017; Kohl 2020), or from (anti)correlated responses to variations in the  
73 environment (e.g. similar or opposite responses to decreased pH). We refer to these  
74 covariations as *microbiota integration* by analogy with the often observed *phenotypic*  
75 *integration* between traits in complex phenotypes (Pigliucci 2003). Such covariations  
76 would indicate constraints in the evolution of microbiota composition.

77

78 Phylogenetic comparative methods offer a rich toolbox for quantifying  
79 phylogenetic signal, reconstructing ancestral states, and detecting integration in  
80 multidimensional phenotypes (Clavel et al. 2015). These methods rely on modeling the  
81 evolution of a set of phenotypic traits across evolutionarily related species through a  
82 multivariate stochastic process, such as the Brownian motion process, running along  
83 the species' phylogenetic tree (Revell et al. 2008; Harmon 2017). The multivariate  
84 Brownian process models the gradual evolution of traits through the accumulation of  
85 stochastic changes drawn from a multivariate normal distribution with a variance-  
86 covariance matrix that reflects the magnitude of the changes for each trait (the variance  
87 terms) and the covariation in the changes between trait pairs (the covariance terms).  
88 This process is relevant to represent long-term variations in the abundances of the  
89 different microbial taxa that constitute the microbiota, as such variations are an  
90 emerging outcome of: (i) the stochastic accumulation of changes in the numerous host  
91 traits that can influence the microbiota, including both extrinsic (e.g. geographic

92 location, habitat) and intrinsic (e.g. diet, antimicrobial excretions) traits (Moran et al.  
93 2019; Kohl 2020; Lim and Bordenstein 2020) and (ii) interactions between microbial  
94 taxa (Foster et al. 2017). Indeed, the Brownian motion process has already been used  
95 to model variations in microbial abundances over host evolutionary time (Capunitan et  
96 al. 2020; Labrador et al. 2021). However, the process is not directly applicable to  
97 compositional data made of relative microbial abundances as it does not constrain its  
98 components to sum to 1, and absolute abundances are unfortunately typically not  
99 provided by mainstream metabarcoding technics used to characterize microbiota  
100 composition. Thus, current phylogenetic comparative methods cannot directly be used  
101 in the context of microbiota evolution without transgressing several model assumptions  
102 (Hird 2019).

103

104 Here, we develop an approach to apply the multivariate Brownian motion  
105 process to compositional data. We also include a widely-used tree transformation  
106 (Pagel 1999) that quantifies phylosymbiosis by evaluating how much host phylogeny  
107 contributes to explaining interspecific variation in present-day microbiota composition.  
108 Phylosymbiosis is typically assessed using correlative approaches such as Mantel  
109 tests (Lim and Bordenstein 2020), which are known to suffer from frequent false  
110 negatives, while process-based approaches such as ours tend to be more powerful  
111 (Harmon and Glor 2010; Hird 2019; Perez-Lamarque, Maliet, et al. 2022). We apply  
112 our new approach to the gut bacterial microbiota of mammals and birds. The gut  
113 microbiota is key to the functioning of their hosts, contributing to their nutrition, their  
114 protection, and their development (McFall-Ngai et al. 2013). Strong phylosymbiosis in  
115 gut bacterial microbiota has been reported for mammals, including primates and  
116 rodents (Ochman et al. 2010; Groussin et al. 2017; Kohl et al. 2018), while it is thought  
117 to be absent for birds, with some exceptions in a few young clades (Song et al. 2020;  
118 Trevelline et al. 2020; Bodawatta et al. 2022). We revisit this dichotomy here, on the  
119 premise that previous analyses may have not been powerful enough to detect  
120 phylosymbiosis in birds (Hird 2019). We analyze potential drivers of phylosymbiotic  
121 patterns, including diet, geographic location, and flying ability, we estimate the  
122 ancestral microbiota composition of mammals and birds, and we investigate patterns  
123 of microbiota integration.

## 124 Results & Discussion:

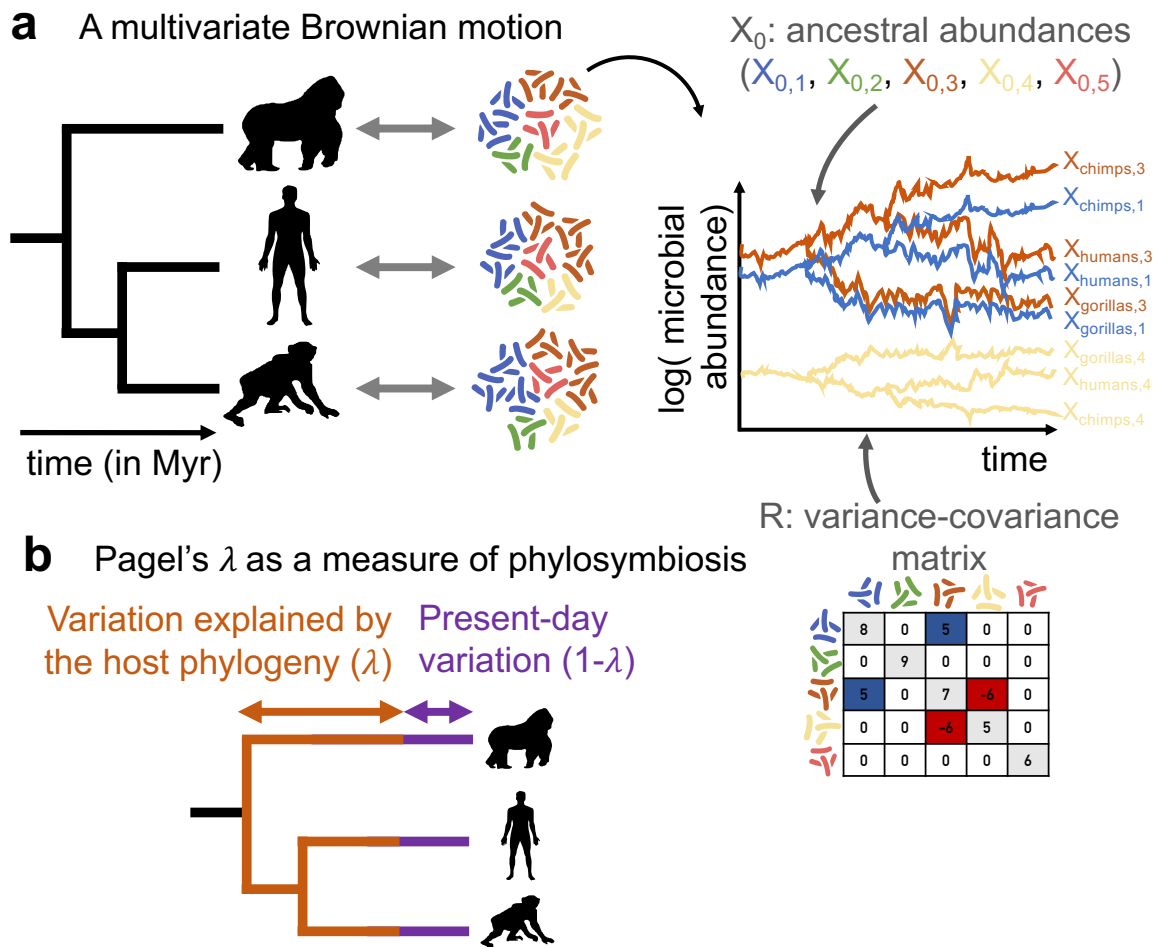
125

126 We developed a method to infer the dynamics of microbiota composition during  
127 host diversification from host-microbiota data (*i.e.* a fixed, bifurcating host phylogeny  
128 and microbiota relative abundances for each extant host species) using the  
129 multivariate Brownian motion process (Figure 1 and Methods). We assume that all  
130 microbial taxa are present in all hosts, potentially in very low (undetectable)  
131 abundances and that they were already present in the most recent common ancestor  
132 of all host species. These assumptions are met if we consider a taxonomic level in the  
133 definition of microbial taxa that is high enough given the host clade, such as bacterial  
134 orders in the vertebrate gut microbiota. We assume that, from ancestral values at the  
135 root  $X_0$ , the log-absolute abundances of the different microbial taxa change on the host  
136 phylogeny following a multivariate Brownian motion model with variance-covariance  
137 matrix  $R$  (Figure 1a). Under this model, the log-absolute abundances fluctuate around  
138 their ancestral values ( $\log X_0$ ) without directional change. In addition, we account for  
139 variation linked to present-day factors by including in the model the widely-used  
140 Pagel's  $\lambda$  transformation of the host phylogenetic tree (Pagel 1999). This  
141 transformation extends the terminal branches of the tree by  $(1-\lambda)$  of the total tree depth  
142 while compressing the internal branches to keep the total tree depth constant, with  $\lambda$   
143 ranging between 0 and 1 (see Figure 1b and Methods).  $\lambda$  estimates close to 1 indicate  
144 that an untransformed tree explains the data quite well, reflecting strong  
145 phylosymbiosis, whereas  $\lambda$  estimates close to 0 indicate that the tree has little  
146 explanatory power, reflecting weak or absent phylosymbiosis. Unlike the traditional  
147 case of the multivariate Brownian motion process applied to phenotypic data, where  
148 the phenotype is directly measured at present, in the case of the microbiota, relative  
149 rather than absolute abundances are measured. To handle this difficulty, we treat total  
150 microbial abundances in each host as latent variables, and sample from the joint  
151 posterior distribution of these latent variables and our parameters of interest: Pagel's  
152  $\lambda$ , which provides us with an estimate of phylosymbiosis, the  $R$  matrix which reflects  
153 microbiota integration, and  $Z_0$ , which indicates the relative microbial abundances in the  
154 ancestral microbiota.

155

156 We tested this inference method on data simulated from our model and found  
157 that we can accurately estimate the ancestral bacterial relative abundances  $Z_0$  (with a  
158 tendency for homogenization) and the variance-covariance matrix  $R$  between microbial  
159 taxa, provided that the number of host species ( $n$ ) and bacterial taxa ( $p$ ) are large  
160 enough ( $n \geq 50$  and  $p \geq 5$ , see Supplementary Results 1). Similarly, the level of  
161 phylosymbiosis  $\lambda$  is accurately estimated for  $p \geq 5$ , and its significance is correctly  
162 inferred for  $n \geq 50$  (see Supplementary Results 1). This approach provides a more  
163 powerful way to detect phylosymbiosis than Mantel tests, which often failed at  
164 detecting low levels of phylosymbiosis ( $0 < \lambda < 0.5$ ; Table S1). This was expected, as  
165 Mantel tests are correlative and are known to suffer from frequent false negatives in

166 comparison with more process-based approaches such as ours (Harmon and Glor  
 167 2010; Hird 2019; Perez-Lamarque, Maliet, et al. 2022).  
 168  
 169



170  
 171  
 172 **Figure 1: A comparative phylogenetic model for the dynamics of microbiota**  
 173 **composition during host diversification:** (a) We model fluctuations in the abundances of  
 174 microbial taxa along a host phylogeny with a multivariate Brownian motion parametrized by  
 175 the ancestral abundances ( $X_0$ ) and the variance-covariance matrix ( $R$ ). The variance terms (on  
 176 the diagonal) reflect the magnitude of the changes, while the covariance terms reflect positive  
 177 or negative covariations in abundances between pairs of microbial taxa. The relative ancestral  
 178 abundances ( $Z_0$ ) and the variance-covariance matrix  $R$  are estimated by adjusting the model  
 179 to the host-microbiota data (host phylogeny and microbiota relative abundances for each host).  
 180 (b) Following the widely-used Pagel's  $\lambda$  transformation, we extend the terminal branches of  
 181 the host phylogenetic tree by  $1-\lambda$  of the total tree depth while compressing the internal  
 182 branches to keep the total tree depth constant.  $\lambda$  is comprised between 0 and 1 and is co-  
 183 estimated during inference.  $\lambda$  close to 1 indicates that closely related hosts tend to have similar  
 184 microbiota due to shared evolutionary history (strong phyllosymbiosis), while  $\lambda$  close to 0  
 185 indicates that microbiota composition is determined by present-day processes with little  
 186 influence of host evolutionary history (weak or absent phyllosymbiosis). The significance of  
 187 phyllosymbiosis is assessed with permutations.

188 We applied our model to the gut bacterial microbiota of 215 mammal species  
189 and 323 bird species from (Song et al. 2020) and found a pervasive signal of  
190 phylosymbiosis. We focused on the 14 most abundant bacterial orders, corresponding  
191 in abundance to 84% and 82% of the total gut bacterial microbiota of mammals and  
192 birds, respectively. We found a markedly higher level of phylosymbiosis in mammals  
193 ( $\lambda \approx 0.65$ ) than in birds ( $\lambda \approx 0.31$ ; Table S2, Figure S1), consistent with previous  
194 literature and our finding that microbiota composition is more species-specific in  
195 mammals than in birds (Table S3). Indeed, bird microbiota is generally more sensitive  
196 to short-term environmental changes such as anthropogenic perturbations or parasite  
197 infections (Bodawatta et al. 2022). By explicitly modeling the non-phylogenetic  
198 component of microbiota composition using a Pagel's  $\lambda$  transformation, we detected a  
199 low but significant level of phylosymbiosis in the gut microbiota of birds (Table S2),  
200 contrary to previous conclusions (Song et al. 2020; Bodawatta et al. 2022) that relied  
201 on Mantel tests.  $\lambda$  values are higher at the level of bacterial phyla (Table S2; Figure  
202 S1), suggesting that microbiota composition is more evolutionarily conserved at higher  
203 taxonomic levels. Testing model performance on data simulated directly on the  
204 mammal and bird phylogenetic trees, we found a low type-I error rate and a high  
205 statistical power, suggesting that the phylosymbiosis we detected in birds is not due to  
206 false detection by our method, but rather to a higher power than previously used  
207 methods (Table S4). Phylosymbiosis is not linked to an effect of captivity nor the  
208 spurious concatenation of different studies either (Supplementary Results 2).  
209 Phylosymbiosis is particularly strong in Primates, Passeriformes, and Cetartiodactyla,  
210 lower but significant in Columbiformes, Chiroptera, and Carnivora, and non-significant  
211 in Rodentia, Charadriiformes, and Anseriformes (Table S2). Non-significant  
212 phylosymbiosis in these orders is likely due to an insufficient number of sampled  
213 species ( $n < 25$ , see Supplementary Results 1). It appears that vertebrate orders with  
214 mainly herbivorous diets have stronger phylosymbiosis, although this would need to  
215 be tested more robustly with a better species coverage (Table S2).

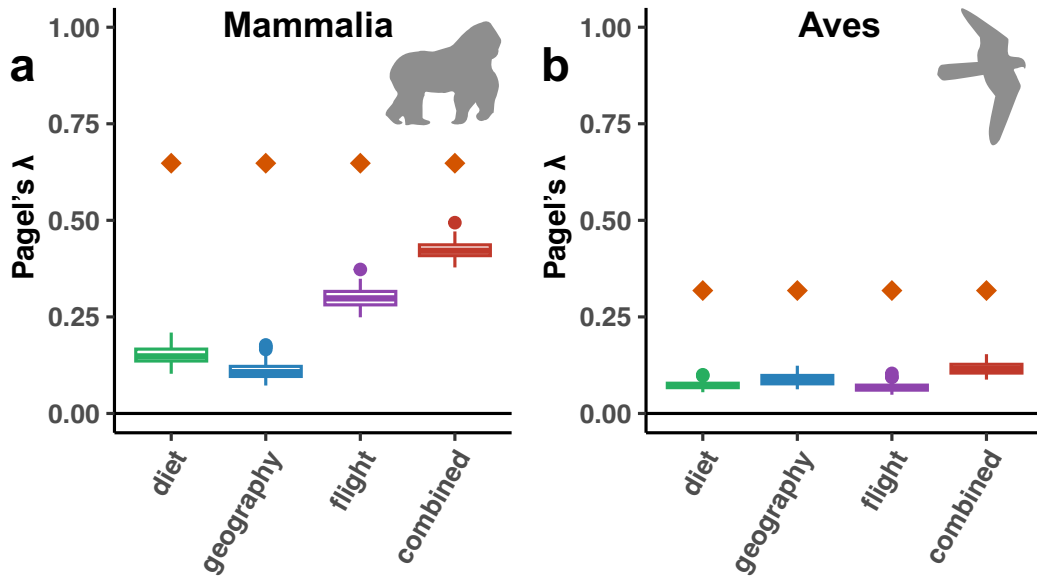
216  
217 Our results suggest that phylosymbiosis is only partially explained by  
218 evolutionary conservatism in flying ability, diet, or geographic location. First, excluding  
219 flying mammals (Chiroptera) or non-flying birds did not impact our estimates of  
220 phylosymbiosis (Table S2). Second, permutation tests shuffling the microbiota of host  
221 species having the same diet, geographic location, flying ability, or combination of  
222 these traits resulted in much lower  $\lambda$  values (Figures 2 & S2). In mammals,  $\lambda$  values  
223 resulting from such shuffling are still significant (Figure 2), suggesting that the  
224 evolutionary conservatism of flying ability, diet, and geographic location contributes to  
225 phylosymbiosis without fully explaining it (Moran et al. 2019). In birds, shuffling often  
226 resulted in non-significant  $\lambda$  values (Figure 2), indicating a weak or absent contribution  
227 of diet or geographic location in the observed phylosymbiosis. Similarly, the  
228 conservatism of these traits is not sufficient to explain the phylosymbiosis measured in  
229 some of the larger mammal and bird clades, such as Primates, Cetartiodactyla, and  
230 Passeriformes (Figure S3). Thus, we suspect that other evolutionary-conserved



231 physiological, immunological, or ecological traits act as host filters (Foster et al. 2017;  
232 Moran et al. 2019) and contribute to phyllosymbiosis in the gut microbiota of mammals  
233 and birds (Goodrich et al. 2016; Mazel et al. 2018).

234

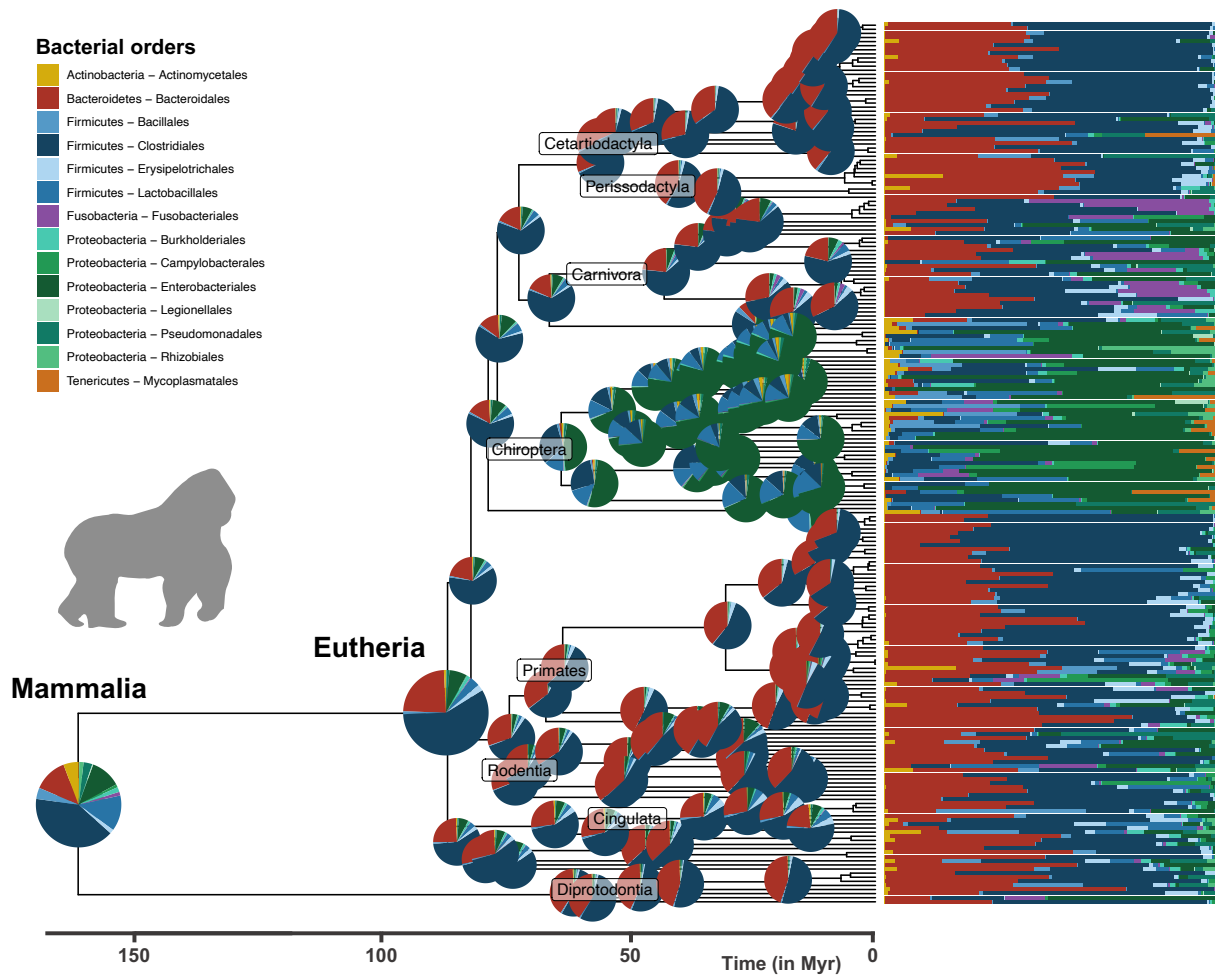
235 Our ancestral reconstructions of the microbiota of early mammals and birds  
236 suggest that Proteobacteria and Firmicutes were much more abundant in the ancestral  
237 gut microbiota of birds than mammals (Figures 3, 4, S4 & S5). As common in  
238 phylogenetic ancestral reconstruction, the uncertainty is quite high (Figure S6); it is  
239 larger in mammals than in birds because of the long branches that separate marsupials  
240 and eutherians at the origin of all mammals. In the absence of fossil constraints,  
241 ancestral reconstructions are a phylogenetically-weighted average of extant  
242 characteristics. Estimated ancestral compositions are thus expectedly close from the  
243 average microbiota compositions of extant bird and mammal species, yet they are  
244 distinct (Figure S7). Comparing the ancestral microbiota composition of mammals to  
245 that of the extant wild mammal species, we found the highest similarity with  
246 invertebrate feeders (distance to the centroid:  $d=1.46$ ), such as the insectivorous  
247 armadillos (*Zaedyus pichiy*), and frugivores ( $d=1.24$ ; Figures 5 & S8; see Methods),  
248 and the lowest similarity with specialist consumers feeding on plants ( $d=2.50$ ) or meat  
249 ( $d=2.82$ ). This result is robust to uncertainty in our estimate of ancestral microbiota  
250 composition (Figure S6b) and when including species sampled in captivity (Figure S7).  
251 Given that mammals originated before fleshy fruit plants (Eriksson 2016), this suggests  
252 that ancestral mammals were generalist invertebrate feeders, which is consistent with  
253 the current hypothesis, based on the fossil record and ancestral diet reconstruction, of  
254 a generalist insectivorous diet in early mammals (Gill et al. 2014; Grossnickle et al.  
255 2019). We found the gut microbiota composition of modern birds to be only weakly  
256 structured by diet compared to that of mammals, making the inferred ancestral  
257 microbiota composition of birds less informative in this respect (no strong clustering in  
258 the PCA plots; PerMANOVA testing the effect of diet:  $R^2\sim 0.03$ ,  $p<0.001$  in birds *versus*  
259  $R^2\sim 0.22$ ,  $p<0.001$  in mammals; Figures 5, S7 & S8; Table S5). In addition, the fact  
260 that, under the assumptions of our model, most extant microbiota compositions in both  
261 mammals and birds remain centered around the estimated ancestral microbiota  
262 composition suggests that only a minority of the extant species experienced major  
263 shifts in their microbiota composition during their evolution.



264  
265

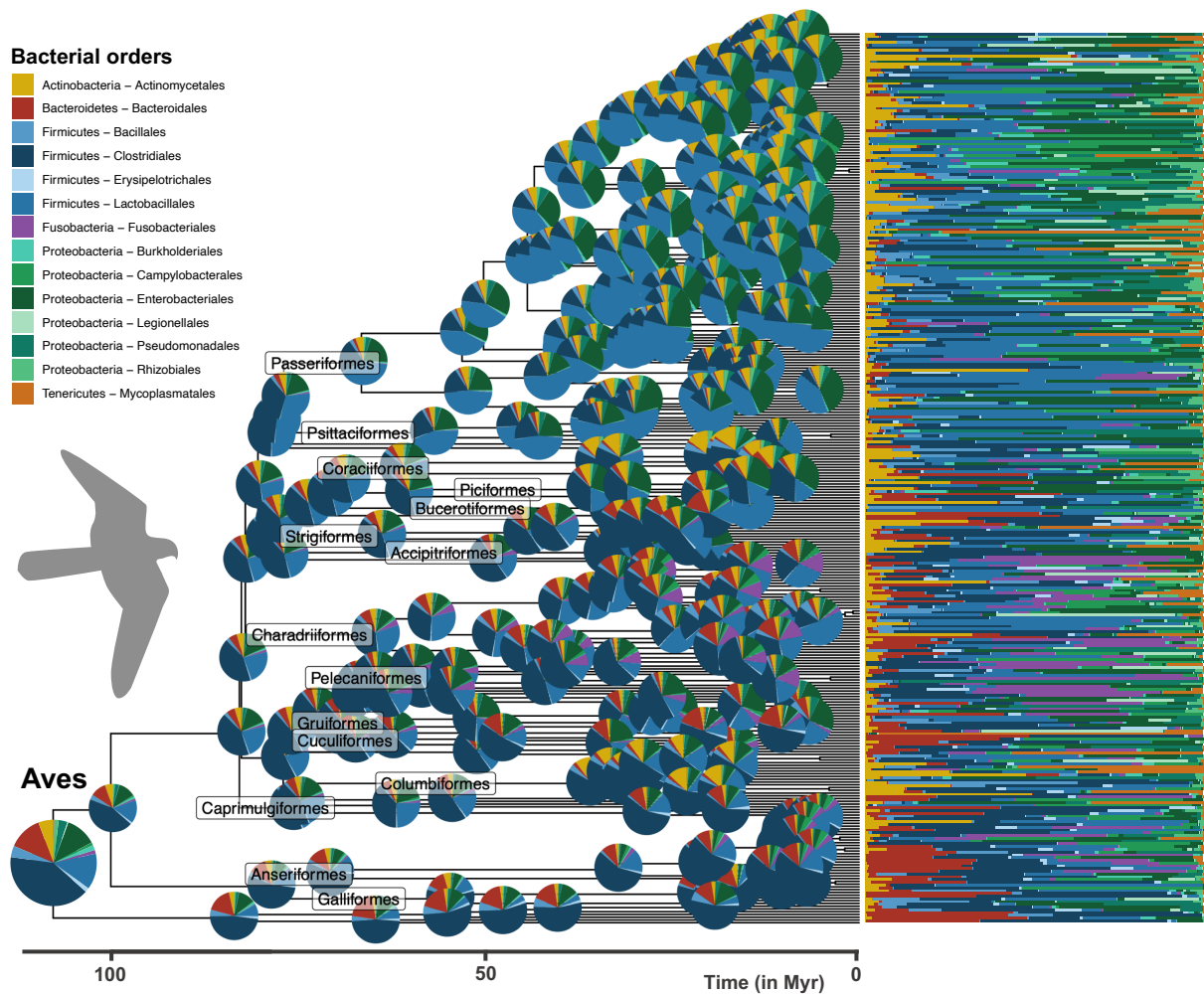
**Figure 2: Phylogenetically-conserved diets, geographic locations, or flying abilities partially contribute to phylosymbiosis in the gut microbiota of mammals, but not birds.**

268 For both mammals and birds, we compared the estimated level of phylosymbiosis (mean  $\lambda$   
269 value in orange) to levels of phylosymbiosis ( $\lambda$  values) estimated when shuffling the species  
270 that have the same diet (green boxplot), geographic location (blue boxplot), flying ability (flying  
271 or non-flying; purple boxplot), or combination of the latter traits (in red). For each shuffling  
272 strategy, we performed 100 randomizations. Combining all traits strongly constrains the  
273 possible permutations, which may consequently retain a phylogenetic signal in the shuffling  
274 and lead to high  $\lambda$  values although the traits are actually not strongly contributing to  
275 phylosymbiosis.



276  
 277  
 278  
 279  
 280  
 281  
 282  
 283

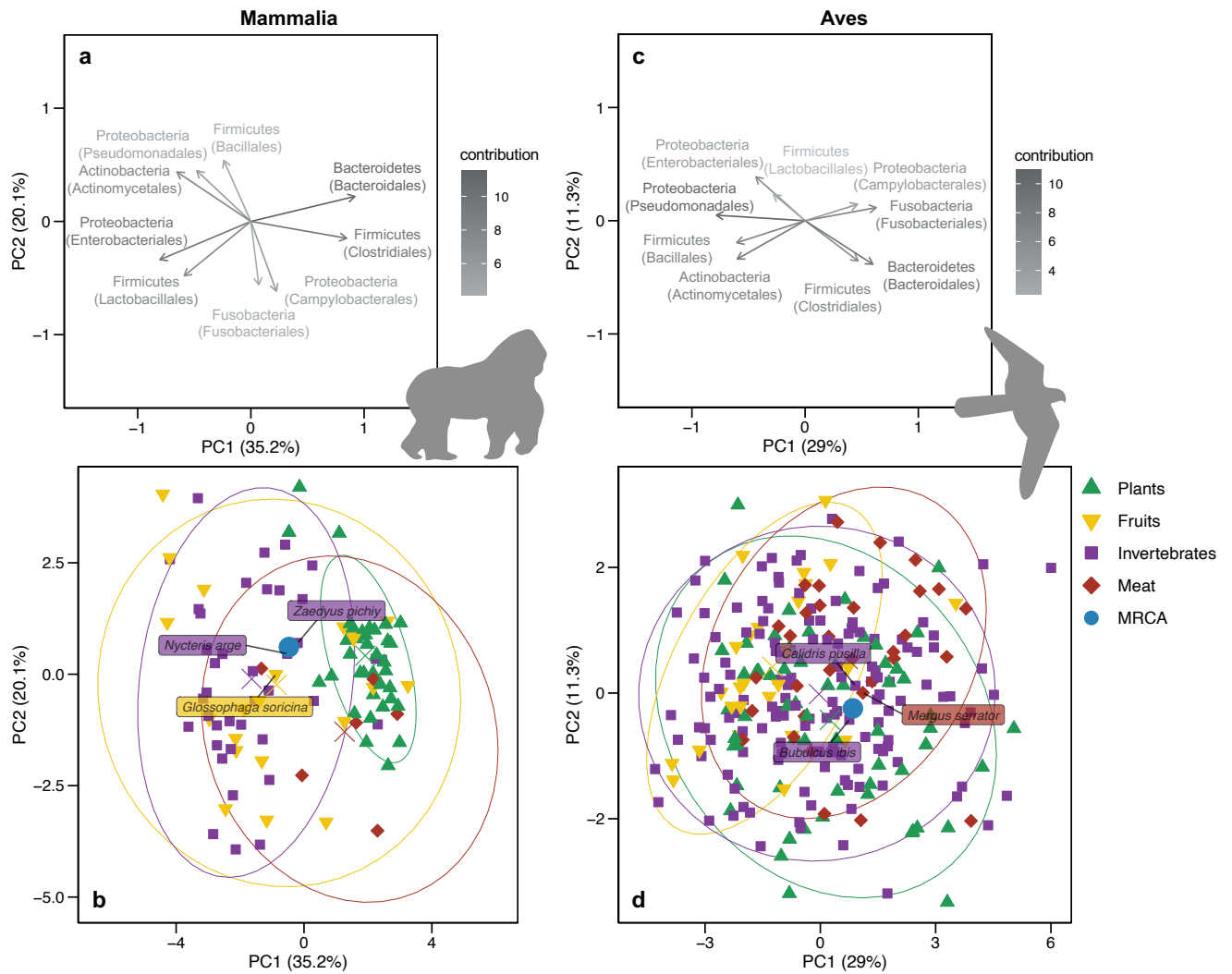
**Figure 3: Ancestral reconstruction of mammalian gut microbiota:** Phylogenetic tree of the sampled mammal species and associated relative abundances of the 14 most abundant bacterial orders (bar charts on the right). Pie charts at the root and nodes of the tree represent estimated ancestral microbiota compositions (mean of the posterior distribution of  $Z_0$  at the root and generalized least squares estimates at other internal nodes). Compositions are not represented at the most recent nodes for the sake of clarity.



284  
 285  
 286  
 287  
 288  
 289  
 290  
 291

**Figure 4: Ancestral reconstruction of avian gut microbiota:** Phylogenetic tree of the sampled birds, and associated relative abundances of the 14 most abundant bacterial orders (bar charts on the right). Pie charts at the root and nodes of the tree represent estimated ancestral microbiota compositions (mean of the posterior distribution of  $Z_0$  at the root and generalized least squares estimates at other internal nodes). Compositions are not represented at the most recent nodes for the sake of clarity.

292 We detected significant changes in microbiota composition in the ancestors of  
293 some mammal and bird orders (Figures 3, 4, & S9). In mammals, the largest shift in  
294 microbiota composition occurred in the ancestor of Chiroptera, with an increased  
295 proportion of Enterobacteriales (Proteobacteria), Mycoplasmatales (Tenericutes), and  
296 to a lesser extent Actinomycetales (Actinobacteria), as well as a decreased proportion  
297 of Bacteroidales (Bacteroidetes), and in Firmicutes, Clostridiales were replaced by  
298 Bacillales and Lactobacillales (Figure 3; Table S6). Other shifts occurred in the  
299 ancestor of Carnivora, with an increased proportion of Fusobacteriales (Fusobacteria),  
300 and in the ancestors of Primates and Cingulata, with an increased proportion of some  
301 Firmicutes orders (*e.g.* Erysipelotrichales; Figures 3 & S9). In addition, Proteobacteria  
302 (especially Enterobacteriales and Pseudomonadales) almost disappeared in the  
303 ancestral microbiota of Ungulata and Simiiformes (New and Old World monkeys; Table  
304 S6). In birds, we found a shift in microbiota composition in the ancestor of  
305 Passeriformes, with more Bacillales and Enterobacteriales, and to a lesser extent  
306 Pseudomonadales, and a quasi-disappearance of Bacteroidales (Figures 4 & S5;  
307 Table S6). The ancestors of Anseriformes and Charadriiforms were characterized by  
308 a larger proportion of Bacteroidales, as well as a large proportion of Fusobacteriales,  
309 often absent or present in low abundances in other bird gut microbiota. Finally, the  
310 relative abundance of Actinomycetales increased in Columbiformes (Table S6). We  
311 found similar estimates of ancestral gut microbiota composition when running separate  
312 inferences for the different mammal and bird orders (Figure S9). Some of these  
313 compositional shifts might be linked to the ecological changes that these lineages  
314 experienced, such as the acquisition of flight for bats or carnivorous diets for Carnivora  
315 and Charadriiforms (Nishida and Ochman 2018; Song et al. 2020).  
316

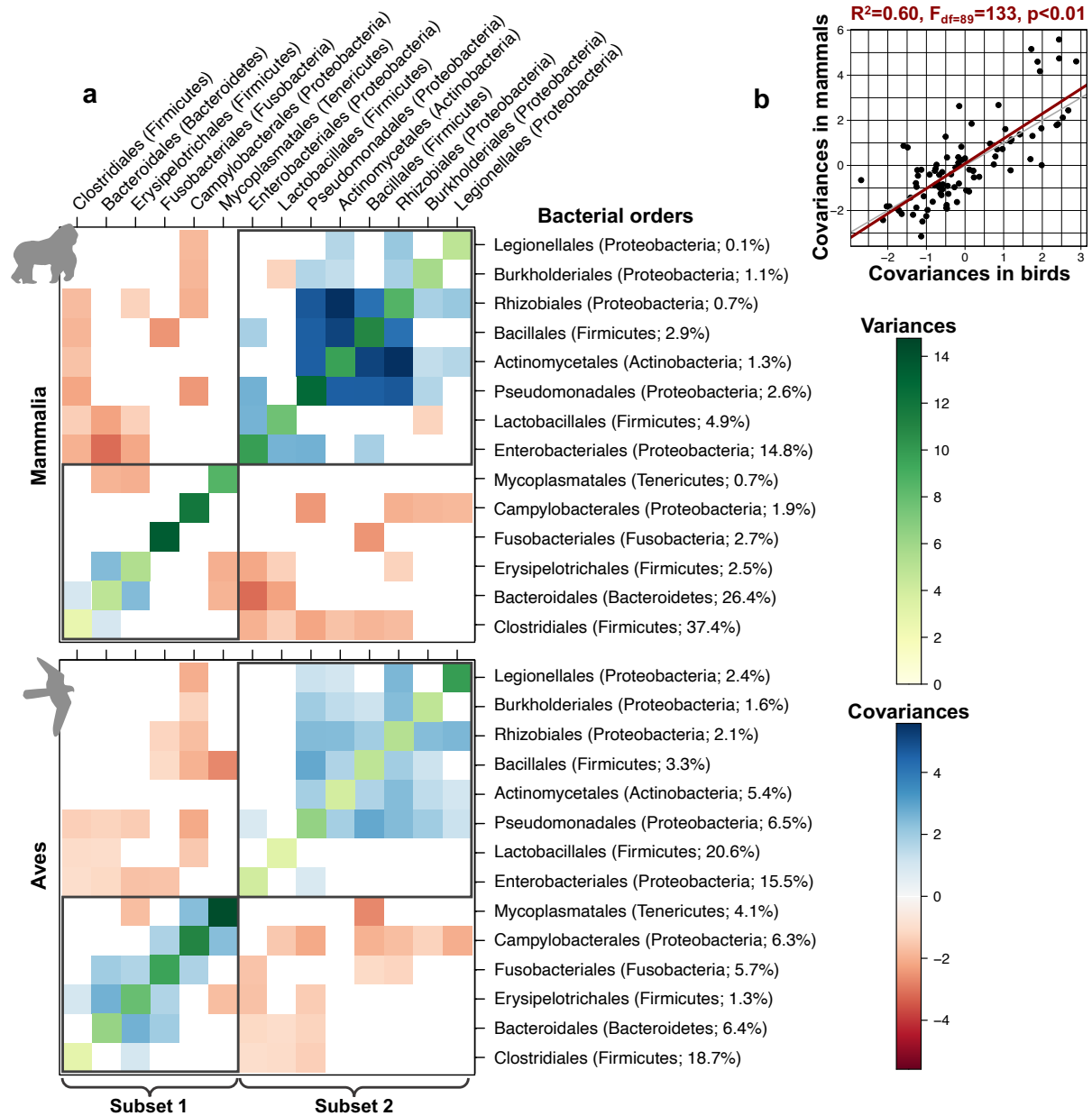


317  
318

319 **Figure 5: Projection of the estimated ancestral gut microbiota of mammals and birds**  
 320 **onto the space of present-day gut microbiota.** Top panels: projection of bacterial orders  
 321 contributing to the two principal components (PC). Colors represent the contribution of the taxa  
 322 to the principal components. Percentages indicate the explained variance of each PC. Only  
 323 the 9 most abundant orders are represented for the sake of clarity. Bottom panels: Projection  
 324 of the extant and ancestral microbiota compositions. Extant microbiota of species sampled in  
 325 the wild are colored according to the species' diet. For each diet, the ellipse contains on  
 326 average 95% of the distribution approximated by a multivariate t-distribution and the centroid  
 327 is indicated by a diagonal cross. Ancestral microbiota compositions of mammals and birds are  
 328 represented in blue. On each PCA plot, we indicated the three extant species with microbiota  
 329 compositions closest to the ancestral microbiota composition. The ancestral gut microbiota of  
 330 mammals is closest to the gut microbiota of present-day invertebrate feeders; the gut  
 331 microbiota of birds does not strongly reflect diet.

332 Far from varying as uncorrelated units during the evolutionary history of  
333 mammals and birds, we found significant covariances between many microbial taxa,  
334 both positive and negative (Figure 6a), suggesting strong constraints in the evolution  
335 of the microbiota. These patterns of microbiota integration are strikingly similar in  
336 mammals and birds (Figure 6b), indicating that they are conserved over long  
337 evolutionary times. Our simulation analyses on the mammal and bird trees suggest  
338 that these results are not artefactual, since we recover significant covariances only  
339 when we include them in the simulations (Table S7, Supplementary Results 1). Similar  
340 covariances were obtained when performing separate inferences on the different  
341 mammal and bird orders (Figure S10), which both confirms our results and suggests  
342 that the model assumption of a constant variance-covariance matrix across the host  
343 phylogenetic tree is reasonable. Combined with the high bacterial variability in time,  
344 across individuals, and across host species at low taxonomic levels, these consistent  
345 patterns at the level of bacterial orders on large time scales suggest that there is a  
346 certain level of functional redundancy among bacteria taxa within orders in the  
347 vertebrate gut microbiota.

348  
349 Both visual inspection and integration analyses of the covariances revealed that  
350 bacterial orders cluster into two main subsets within which taxa tend to covary in a  
351 concerted way, while taxa from different subsets tend to be anti-correlated (Figure 6;  
352 see Methods). The first subset (“subset 1”) is formed in particular by the orders  
353 Clostridiales, Bacteroidales, and Fusobacteriales, and the second subset (“subset 2”)  
354 is mainly composed of the orders Enterobacteriales, Lactobacillales, Pseudomonades,  
355 Actinomycetales, and Bacillales. Although some host species have a microbiota  
356 composed of an even mixture of these two bacterial subsets, one subset generally  
357 prevails, leading to the existence of two main gut microbiota profiles. The first subset  
358 is dominant in the microbiota of most mammals (excluding Chiroptera), the ancestors  
359 of birds, and some extant bird lineages (*e.g.* Anseriformes, Columbiformes, or  
360 Accipitriformes); the second subset predominates in the microbiota of Chiroptera and  
361 other bird lineages, including Passeriformes (Figure S11). This result suggests the  
362 existence of two main gut microbiota profiles conserved over millions of years across  
363 vertebrates.



364

365

366

367

368

369

370

371

372

373

374

**Figure 6: Estimated variances and covariances between the main bacterial taxa tend to be similar in the gut microbiota of mammals and birds. (a)** For each variance-covariance matrix between bacterial taxa estimated using our model of host microbiota evolution, we represented negative covariances in red and positive covariances in blue, while variances are represented in shades of green. Non-significant covariances are represented in white. Grey rectangles correspond to subsets of bacterial orders that tend to covary positively. **(b)** Correlation between covariances between the main bacterial taxa estimated in the gut microbiota of mammals or birds. The red line indicates the corresponding linear model, while the grey line corresponds to  $y=x$ .



375 We can only speculate on the processes underlying positive or negative  
376 covariances between bacterial orders: we cannot distinguish from our analyses  
377 whether they indicate direct interactions between bacterial taxa (e.g. cross-feeding or  
378 competition) or indirect interactions mediated by similar/opposed microbial responses  
379 to changes in the gut environment. For instance, the frequent and strong negative  
380 covariations observed between the abundant Enterobacteriales (Proteobacteria) and  
381 the major bacterial orders Clostridiales (Firmicutes) and Bacteroidales (Bacteroidetes)  
382 may result from direct competitions (Shealy et al. 2021), host immunological controls  
383 over Proteobacteria (Mirpuri et al. 2013), and/or be mediated by the oxygen  
384 concentration in the gut, as Proteobacteria are facultative anaerobes, while other phyla  
385 are obligate anaerobes (Shin et al. 2015). The strongest positive covariations we  
386 inferred between Actinomycetales, Pseudomonadales, and Rhizobiales, which are the  
387 most abundant bacterial orders in plant tissues (Wagner et al. 2016), may reflect a  
388 plant-based diet, which would lead to a concomitant increase of plant-associated  
389 bacteria in the gut microbiota of herbivorous vertebrates (Dion-Phénix et al. 2021).  
390 Some of the covariations we detected (e.g. the negative covariation between  
391 Lactobacillales and Bacteroidales) have also been observed in human microbiome  
392 data using co-occurrence network analyses (Faust et al. 2012), suggesting that at least  
393 some covariations between microbial taxa that occur over short timescales within host  
394 species are conserved over macroevolutionary timescales.

395  
396 To test the adequacy of our model to the data, we simulated microbiota under  
397 our model using the parameters estimated on mammal and bird data. We found that  
398 simulated microbiota have compositions similar to those observed in extant mammals  
399 and birds (Figure S12), which indicates that, despite its simple assumptions, our  
400 multivariate Brownian motion model generates realistic gut microbiota (Hird 2019;  
401 Labrador et al. 2021). Nevertheless, the gut microbiota composition of mammals and  
402 birds appears more constrained than the sets of compositions we can simulate using  
403 multivariate Brownian motions (Figure S12). This is particularly true for mammals and  
404 may be linked to constraints that are not accounted for by our model, such as selective  
405 pressures toward particular microbiota compositions, the potential existence of  
406 carrying capacities for some bacterial orders, or non-constant or non-homogeneous  
407 variance-covariance matrices (e.g., more frequent shifts in microbiota composition  
408 early in clades history, effects of host traits such as diet or gut pH on covariation).  
409 Extensions of our multivariate Brownian motion approach could accommodate such  
410 constraints, but this may complexify inferences. We hope that this work will foster the  
411 development of more complex models that may better represent microbiota evolution  
412 in systems that present non-Brownian behaviors. As a first step, extensions that relax  
413 the constant variance assumption (e.g., the early-burst model; Harmon et al. 2010)  
414 would be relatively straightforward to implement and could be particularly relevant to  
415 account for the major shifts in microbiota composition that took place at the origin of  
416 some mammalian orders (e.g., in bats). Meanwhile, by relying on a simple and flexible  
417 Brownian motion process, our phylogenetic comparative model for microbiota

418 evolution is general enough to be broadly applied across other host-microbiota  
419 systems and reveal the global trends of microbiota evolution.

420

421 Besides modeling assumptions, our results may be influenced by the inherent  
422 biases of metabarcoding data. Bacterial relative abundances characterized using  
423 metabarcoding techniques are a distortion of the actual relative abundances (Knight et  
424 al. 2018; Lavrinienko et al. 2021), since metabarcoding is sensitive to the number of  
425 rRNA copies in the bacterial genomes, primer biases, and the quality and  
426 completeness of the reference database for taxonomic assignment (at the bacterial  
427 order/phylum level in our case). These issues are unlikely to artefactually generate  
428 phylosymbiosis or covariations across bacterial taxa because we expect such biases  
429 to be homogeneous across host species; nevertheless, they are likely to affect our  
430 ancestral reconstructions of microbiota compositions.

431

432 Our approach to quantifying phylosymbiosis characterizes microbiota  
433 composition in terms of the relative abundances of higher bacterial taxa (orders or  
434 phyla). This characterization hides variations in the presence/absence of bacterial taxa  
435 at lower taxonomic levels (e.g. genus or species). Indeed, distinct mammal or bird  
436 species are known to host different bacterial species (Song et al. 2020), and this may  
437 not translate into abundance variations at higher taxonomic levels if the different  
438 bacterial species belong to the same higher taxa. Besides the widely-used Mantel  
439 tests, such variations could be accounted for by stochastic processes modeling the  
440 evolution of presence/absence on host phylogenies (Braga et al. 2020), although we  
441 are not aware that these approaches have been used to detect bacterial  
442 phylosymbiosis. Yet another level of variation in microbiota composition that can  
443 contribute to phylosymbiosis arises through genetic differentiation below the bacterial  
444 species level: if a bacterial species is vertically transmitted during host diversification,  
445 we expect bacterial strains from closely related host species to be more genetically  
446 similar (Sanders et al. 2014; Groussin et al. 2017; Perez-Lamarque and Morlon 2019).  
447 This latter process can be specifically tested thanks to cophylogenetic methods that  
448 consider the evolution of each microbial species separately (Dismukes et al. 2022;  
449 Perez-Lamarque and Morlon 2022). The above-mentioned methods are  
450 complementary, as they focus on different levels of variations in microbiota  
451 composition, and on the distinct processes that simultaneously generate  
452 phylosymbiosis (Moran et al. 2019; Lim and Bordenstein 2020).

453

454 Phylosymbiosis is a widespread pattern that has fascinated microbial ecologists  
455 and evolutionary biologists since its discovery, spurring debates on the main processes  
456 underlying the pattern. Drawing upon phylogenetic comparative methods, we have  
457 developed a new approach to studying phylosymbiosis. Our results on simulations and  
458 birds suggest that phylosymbiosis may be even more prevalent than currently  
459 recognized, but sometimes undetected with correlative approaches. We have shown  
460 that conservatisms in diet, geographic location, and flying ability are not enough to  
461 explain phylosymbiosis, calling for an investigation of the role of other host ecological

462 traits, as well as physiological and immunological traits. One of our most striking  
463 results, in the face of the well-known high variability of the gut microbiota, is its high  
464 level of integration, with conserved covariations between bacterial orders over millions  
465 of years. The same two subsets of bacterial orders tend to covary in a concerted way  
466 in both mammals and birds, leading to the existence of two main gut microbiota profiles  
467 in vertebrates. Hence, microbial interactions combined with phylogenetically-  
468 conserved host traits shape microbiota composition over millions of years, supporting  
469 the view of vertebrate gut microbiota as 'ecosystems on a leash' (Foster et al. 2017).

470 **Methods:**

471

472 **A multivariate Brownian motion model for variations in microbiota composition**  
473 **over host evolutionary time:**

474

475 We denote by  $p$  the total number of microbial taxa detected across the  
476 microbiota of the  $n$  sampled host species. Standard metabarcoding techniques only  
477 measure the relative abundance of each microbial taxon  $j$  in each extant host species  
478  $i$ , which we denote by  $Z_{ij} = X_{ij}/Y_i$ , where  $X_{ij}$  is the unmeasured absolute abundance  
479 of microbial taxon  $j$  in host  $i$  and  $Y_i = \sum_j X_{ij}$  is the unmeasured total microbial  
480 abundance in the microbiota of host  $i$ . We assume that the logarithms of microbial  
481 absolute abundances  $\log X_{ij}$  vary along the host phylogenetic tree according to a  
482 multivariate Brownian motion starting from the ancestral abundances at the root,  
483 denoted by  $X_{0j}$  (Figure 1). Indeed, taking the logarithm of the abundances yields values  
484 on the real axis that are amenable to be modeled with a Brownian motion, similar to  
485 continuous phenotypic traits. This model implies a log-normal distribution of  
486 abundances, as is commonly observed in microbial communities (Quince et al. 2008),  
487 and it can easily accommodate undetected microbial taxa in some hosts by assigning  
488 them very low unobserved relative abundances. To make the model identifiable, we  
489 express the total abundances  $Y_i$  relative to the unknown total abundance at the root  $Y_0$ ,  
490 and we only infer  $\tilde{Y}_i = Y_i/Y_0$ . Each microbial taxon  $i$  is characterized by a certain  
491 variance and pairs of microbial taxa can affect each other through a covariance term,  
492 so that their changes in abundance over time can be positively or negatively correlated.  
493 All variance and covariance values are assumed to be constant along the host  
494 phylogeny and are summarized by the invertible variance-covariance matrix  $R$  (Figure  
495 1a).

496

497 **Model inference:**

498

499 To infer the model parameters, we sampled from their joint posterior distribution  
500  $P(\log Z_0, R, \lambda, \log \tilde{Y}_1, \dots, \log \tilde{Y}_n | Z_{11}, \dots, Z_{ij}, \dots, Z_{np}, C)$  using a No U-turn Hamiltonian  
501 Monte Carlo sampler, a computationally efficient Markov Chain Monte Carlo algorithm  
502 for continuous variables (Supplementary Methods 1). We implemented it in the  
503 probabilistic programming language Stan and we ran and compiled it through the  
504 RStan interface (R Core Team 2022; Stan Development Team 2022). Inferences were  
505 performed with 4 independent chains and a minimum of 4,000 iterations per chain  
506 including a warmup of 2,000 iterations. We checked the convergence of the chains  
507 using the Gelman statistics and effective sample sizes (ESS). We extracted the mean  
508 posterior value of each parameter and its associated 95% credible interval across  
509 posterior samples.

510

511 We considered a covariance to be significant if 0 was not included in its 95%  
512 credible interval. We could not use the same approach for  $\lambda$ , because it only takes

513 positive values. Furthermore, model selection using Bayes factors led to many false  
514 negatives on simulated data (Supplementary Methods 2 & Results 1). Therefore, we  
515 assessed the significance of  $\lambda$  using permutations. We shuffled at random the extant  
516 host species to break the phylogenetic structure and ran again model inference of the  
517 randomized dataset. We performed 100 replications and compared the distribution of  
518  $\lambda$  values thus obtained to the original  $\lambda$  estimate: if the original  $\lambda$  was greater than at  
519 least 95% of the  $\lambda$  values obtained through permutations, we considered that there  
520 was a significant impact of host evolution on microbiota evolution.

521

## 522 **Simulations:**

523

524 We evaluated our approach using simulations. We simulated the evolution of a  
525 microbiota along a host phylogeny using Multivariate Brownian motions for log-  
526 abundances. We simulated phylogenies with  $n = 20, 50, 100,$  or  $250$  extant host  
527 species using a pure birth model (*pbtree* function in the phytools R-package (Revell  
528 2012)). We considered microbiota with  $p = 3, 5, 10,$  or  $15$  microbial taxa and uniformly  
529 sampled the logarithms of their ancestral abundances at the root of the host phylogeny  
530 between  $-4$  and  $0$  before normalizing them so that  $\sum_j Z_{0j} = 1$ . We generated random  
531 positive definite variance-covariance matrices  $R$  following (Uyeda et al. 2015) and  
532 (Clavel et al. 2019) with eigenvalues of  $1/4$ . Finally, we applied Pagel's  $\lambda$   
533 transformations with  $\lambda = 1, 0.75, 0.5, 0.25,$  or  $0$ . For each combination of  $n, p,$  and  $\lambda$   
534 values, we performed 100 independent simulations, leading to a total of 8,000  
535 simulations. We verified that our approach correctly estimates the parameters  $\lambda, Z_0,$   
536 and  $R$ , and detects phylosymbiosis (significant  $\lambda$ ) and covariations (significant  $R$   
537 components) when they are simulated. We compared the performances of our  
538 approach for detecting phylosymbiosis to that of Mantel tests (Perez-Lamarque, Maliet,  
539 et al. 2022).

540

541 We also evaluated our inference approach using data simulated on the  
542 phylogenetic tree of mammals or birds, and using conditions and parameters matching  
543 the empirical data. We performed simulations with 7 taxa (corresponding to the 7  
544 bacterial phyla in the data, see below) and 14 taxa (corresponding to the 14 bacterial  
545 orders in the data). We used values of  $\lambda = 1, 0.75, 0.5, 0.25,$  or  $0$ , and values for the  
546 other model parameters similar to those estimated from the empirical data (Figure  
547 S13). We performed 100 simulations per condition (thus reaching a total of 2,000  
548 simulations).

549

## 550 **Empirical application:**

551

552 We downloaded the dataset of (Song et al. 2020) that gathered the gut microbiota of  
553 2,677 mammal individuals from  $>200$  species and 1,630 bird individuals from  $>300$   
554 species, characterized by metabarcoding using the V4 region of the 16S rRNA gene.  
555 Only studies using the standard protocol of the Earth Microbiome Project (Thompson

556 et al. 2017) were included (see (Song et al. 2020) for details), making samples  
557 comparable across different studies (Knight et al. 2018). Song *et al.* converted bacterial  
558 reads into amplicon sequence variants (ASV), assigned each ASV taxonomically using  
559 the Greengenes database (DeSantis et al. 2006; Song et al. 2020), and rarefied ASV  
560 tables at 10,000 reads per sample. We complemented their dataset with the consensus  
561 phylogenetic trees of (Upham et al. 2019) and (Jetz et al. 2012) for mammals and  
562 birds, respectively. We only kept the species having their microbiota compositions  
563 characterized by at least 2 microbiota samples (Table S2). We checked that gut  
564 microbiota from the same host species were more similar than gut microbiota from  
565 different species using PerMANOVA (Oksanen et al. 2016). Then, we obtained the  
566 microbiota composition of each host species by averaging the samples per species  
567 and extracted the relative abundances of the main bacterial orders and phyla per host  
568 species. We verified that similar results were obtained when repeating our analyses by  
569 randomly sampling one individual per host species (Figure S14). We only considered  
570 the 14 most abundant bacterial orders, *i.e.* those that each represented more than 1%  
571 of the total bacterial abundance (which correspond in abundance to 84% and 82% of  
572 the total gut bacterial microbiota of mammals and birds, respectively) and the 7 most  
573 abundant bacterial phyla (95% and 96% of the gut microbiota of mammals and birds  
574 respectively; Figure S15). We also repeated all analyses using only the 9 (resp. 5)  
575 most abundant orders (resp. phyla). We did not apply our model at lower taxonomic  
576 levels mainly because the assumptions of our model (all microbial taxa are present in  
577 all hosts, potentially in undetectable abundances and they were already present in the  
578 most recent common ancestor of all host species) are more likely to be met at high  
579 taxonomic levels. At lower taxonomic levels, the microbiota evolution of mammals and  
580 birds may be better represented using models of colonization and extinction (Song et  
581 al. 2020) than models of fluctuations in bacterial abundances such as ours. In addition,  
582 running the model with several hundreds of taxa would be computationally intensive.  
583 Finally, the quality of the taxonomic assignation and the number of taxa representing  
584 more than 1% of the gut microbiota decreased sharply at low taxonomic levels: only  
585 81% and 45% of the gut microbiota of mammals and birds are assigned at the family  
586 and genus levels, respectively, and among them, only 60% and 18% of the bacterial  
587 taxa represent more than 1% of the gut microbiota.

588  
589 Our multivariate Brownian motion model of microbiota does not explicitly  
590 consider losses of bacterial taxa from the microbiota through time. Yet, some bacterial  
591 taxa can be absent or undetected in the gut microbiota of mammals and birds. We  
592 assumed that the absence of a particular taxon came from a very low abundance,  
593 below the detection threshold: we thus arbitrarily set the relative abundances of absent  
594 taxa to 0.001%. Setting the minimal relative abundances of absent taxa to 0.01%  
595 reduced the estimated variance of the rare taxa but did not affect other estimates  
596 (Figure S16).

597

598 We applied the model separately on all mammals and all birds, getting estimates  
599 of Pagel's  $\lambda$ , the ancestral microbiota composition  $Z_0$ , and the variance-covariance  
600 matrix  $R$  for each vertebrate class.

601

### 602 **Effect of host traits on phylosymbiosis:**

603

604 We gathered data on host species traits from (Song et al. 2020) for diet,  
605 geographic location, and flying ability. We assigned a dominant diet to each host  
606 species as either "plants", "fruits", "invertebrates" or "meat" following the EltonTraits  
607 database (Wilman et al. 2014). We assigned a geographic location to each species by  
608 picking the biogeographic realm (Afrotropical, Antarctic, Australasian, Nearctic,  
609 Neotropic, Oriental, or Palearctic) where the highest number of wild individuals were  
610 sampled, or if not available, where the highest number of captive individuals were  
611 sampled (this was the case for 48% of the mammalian species and 18% of the avian  
612 ones). We treated flying ability as binary (yes/no). First, we assessed the influence of  
613 flight on the gut microbiota by performing inferences on non-flying mammal species  
614 only (*i.e.* excluding bats) and on flying bird species only. Similarly, we investigated the  
615 effect of captivity on our inferences by replicating them using only the gut microbiota  
616 of wild or captive individuals. Second, we tested whether the evolutionary conservatism  
617 of diet, geographic location, or flying ability may explain phylosymbiosis in mammals  
618 and birds by performing permutations. We shuffled host species having the same diet,  
619 geographic location, and/or flying ability and re-ran the inferences on these  
620 randomized datasets. For each tested trait, we performed 100 independent  
621 randomizations. Finally, we verified that phylosymbiosis did not artefactually arise from  
622 the concatenation of the separate studies composing this dataset by randomizing the  
623 species that came from the same study.

624

### 625 **Comparison between ancestral and present-day microbiota composition:**

626

627 We compared the estimated ancestral microbiota composition  $Z_0$  of all  
628 mammals or birds to that of extant species using principal component analysis (PCA)  
629 after applying a centered log-ratio transform to the abundances (Aitchison 1983).  
630 Given  $Z_0$ , we also jointly estimated the ancestral abundances at each node of the host  
631 phylogenetic tree using generalized least squares following (Martins and Hansen 1997;  
632 Cunningham et al. 1998; Clavel et al. 2019). As a first attempt to infer past diet based  
633 on the estimated ancestral microbiota composition  $Z_0$ , we computed the centroid of  
634 each of the four diet categories and computed the distance  $d_i$  between  $Z_0$  and each  
635 centroid on the first five PC axes. We additionally performed separate model inference  
636 for all orders of mammals (Carnivora, Cetartiodactyla, Chiroptera, Primates, and  
637 Rodentia; Table S2) and birds (Anseriformes, Charadriiformes, Columbiformes, and  
638 Passeriformes) represented by at least 15 species, and compared the ancestral  
639 microbiota composition obtained with separate and joint inferences.

640

641 **Integration analyses:**

642

643 We identified the significantly positive or negative covariances between  
644 bacterial orders. In addition, to characterize potential subsets of bacterial taxa that tend  
645 to vary in a concerted way, we clustered taxa using the *cluster\_fast\_greedy* function in  
646 the R-package igraph (Csardi and Nepusz 2006), based on the estimated variance-  
647 covariance matrix  $R$ , modified to retain information of only positive covariances  
648 (negative ones were set to 0).

649

650 **Model adequacy:**

651

652 To assess whether our model for the evolution of the gut microbiota of mammals and  
653 birds yields realistic microbiota compositions, we simulated the process of microbiota  
654 evolution on the mammal or bird phylogenies using the parameters estimated for  
655 mammals and birds ( $\log Z_0$ ,  $R$ , and  $\lambda$ ). Next, we compared the simulated microbiota  
656 compositions to the empirical microbiota compositions of the extant mammal or bird  
657 species using principal component analysis (PCA). We performed 20 independent  
658 simulations for each of our model inferences.

659

660 **Data availability:**

661

662 Raw data and processed data from (Song et al. 2020) used to perform the empirical  
663 applications are available in Qiita (<https://qiita.ucsd.edu/study/description/11166>).

664 Our phylogenetic comparative method, referred to as ABDOMEN (A Brownian moDel  
665 Of Microbiota Evolution), is available on GitHub with a tutorial:  
666 <https://github.com/BPerezLamarque/ABDOMEN>.

667

668 **Acknowledgments:**

669

670 The authors acknowledge Julien Clavel, Jonathan Drury, Félix Foutel--Rodier, and  
671 members of the BioDiv team at IBENS for helpful discussions, as well as the Editor  
672 Aurélien Tellier and two anonymous reviewers for their constructive comments. They  
673 also acknowledge the Hubert Curien Alliance program for funding workshops that  
674 initiated the project. GSK acknowledges support from the Academy of Finland  
675 (decision 340314) and the Sakari Alhopuro foundation (grant 20210172). This work  
676 was performed using HPC resources from GENCI-IDRIS (Grants 2021-A0100312405  
677 and 2022- AD010313735).

678

679 **Author Contributions:**

680

681 BPL, GSK, LD, and HM designed the study. BPL and GSK implemented the model.  
682 BPL performed the simulations and the empirical applications. BPL, GSK, and HM  
683 wrote the manuscript.



684

685 **Declaration of interests:**

686

687 The authors declare no competing interests.

688

689 **References:**

690

691 Aitchison J. 1983. Principal component analysis of compositional data. *Biometrika*  
692 70:57.

693 Amato KR, G. Sanders J, Song SJ, Nute M, Metcalf JL, Thompson LR, Morton JT,  
694 Amir A, J. McKenzie V, Humphrey G, et al. 2019. Evolutionary trends in host  
695 physiology outweigh dietary niche in structuring primate gut microbiomes. *ISME*  
696 *J.* 13:576–587.

697 Bodawatta KH, Hird SM, Grond K, Poulsen M, Jønsson KA. 2022. Avian gut  
698 microbiomes taking flight. *Trends Microbiol.* 30:268–280.

699 Braga MP, Landis MJ, Nylín S, Janz N, Ronquist F. 2020. Bayesian inference of  
700 ancestral host-parasite interactions under a phylogenetic model of host  
701 repertoire evolution. *Syst. Biol.* 69:1149–1162.

702 Brooks AW, Kohl KD, Brucker RM, van Opstal EJ, Bordenstein SR. 2016.  
703 *Phylosymbiosis: relationships and functional effects of microbial communities*  
704 *across host evolutionary history.* Relman D, editor. *PLOS Biol.* 14:e2000225.

705 Capuntan DC, Johnson O, Terrill RS, Hird SM. 2020. Evolutionary signal in the gut  
706 microbiomes of 74 bird species from Equatorial Guinea. *Mol. Ecol.* 29:829–847.

707 Clavel J, Aristide L, Morlon H. 2019. A penalized likelihood framework for high-  
708 dimensional phylogenetic comparative methods and an application to New-  
709 World monkeys brain evolution. *Syst. Biol.* 68:93–116.

710 Clavel J, Escarguel G, Merceron G. 2015. mvMORPH: An R package for fitting  
711 multivariate evolutionary models to morphometric data. Poisot T, editor. *Methods*  
712 *Ecol. Evol.* 6:1311–1319.

713 Csardi G, Nepusz T. 2006. The igraph software package for complex network  
714 research. *InterJournal Complex Syst. Complex Sy:*1695.

715 Cunningham CW, Omland KE, Oakley TH. 1998. Reconstructing ancestral character  
716 states: a critical reappraisal. *Trends Ecol. Evol.* 13:361–366.

717 David LA, Maurice CF, Carmody RN, Gootenberg DB, Button JE, Wolfe BE, Ling A  
718 V., Devlin AS, Varma Y, Fischbach MA, et al. 2014. Diet rapidly and reproducibly  
719 alters the human gut microbiome. *Nature* 505:559–563.

720 DeSantis TZ, Hugenholtz P, Larsen N, Rojas M, Brodie EL, Keller K, Huber T, Dalevi  
721 D, Hu P, Andersen GL. 2006. Greengenes, a chimera-checked 16S rRNA gene  
722 database and workbench compatible with ARB. *Appl. Environ. Microbiol.*  
723 72:5069–5072.

724 Dion-Phénix H, Charmantier A, de Franceschi C, Bourret G, Kembel SW, Réale D.  
725 2021. Bacterial microbiota similarity between predators and prey in a blue tit  
726 trophic network. *ISME J.* 15:1098–1107.

727 Dismukes W, Braga MP, Hembry DH, Heath TA, Landis MJ. 2022. Cophylogenetic  
728 methods to untangle the evolutionary history of ecological interactions. *Annu.*  
729 *Rev. Ecol. Evol. Syst.* 53:1–24.

730 Eriksson O. 2016. Evolution of angiosperm seed disperser mutualisms: The timing of  
731 origins and their consequences for coevolutionary interactions between

732 angiosperms and frugivores. *Biol. Rev.* 91:168–186.

733 Faust K, Sathirapongsasuti JF, Izard J, Segata N, Gevers D, Raes J, Huttenhower C.  
734 2012. Microbial co-occurrence relationships in the human microbiome. Ouzounis  
735 CA, editor. *PLoS Comput. Biol.* 8:e1002606.

736 Foster KR, Schluter J, Coyte KZ, Rakoff-Nahoum S. 2017. The evolution of the host  
737 microbiome as an ecosystem on a leash. *Nature* 548:43–51.

738 Gill PG, Purnell MA, Crumpton N, Brown KR, Gostling NJ, Stampanoni M, Rayfield  
739 EJ. 2014. Dietary specializations and diversity in feeding ecology of the earliest  
740 stem mammals. *Nature* 512:303–305.

741 Goodrich JK, Davenport ER, Waters JL, Clark AG, Ley RE. 2016. Cross-species  
742 comparisons of host genetic associations with the microbiome. *Science* (80- ).  
743 352:532–535.

744 Grossnickle DM, Smith SM, Wilson GP. 2019. Untangling the multiple ecological  
745 radiations of early mammals. *Trends Ecol. Evol.* 34:936–949.

746 Groussin M, Mazel F, Sanders JG, Smillie CS, Lavergne S, Thuiller W, Alm EJ. 2017.  
747 Unraveling the processes shaping mammalian gut microbiomes over  
748 evolutionary time. *Nat. Commun.* 8:14319.

749 Hacquard S, Garrido-Oter R, González A, Spaepen S, Ackermann G, Lebeis S,  
750 McHardy AC, Dangl JL, Knight R, Ley R, et al. 2015. Microbiota and host  
751 nutrition across plant and animal kingdoms. *Cell Host Microbe* 17:603–616.

752 Harmon LJ. 2017. *Phylogenetic Comparative Methods*.

753 Harmon LJ, Glor RE. 2010. Poor statistical performance of the Mantel test in  
754 phylogenetic comparative analyses. *Evolution* (N. Y). 64:2173–2178.

755 Harmon LJ, Losos JB, Jonathan Davies T, Gillespie RG, Gittleman JL, Bryan  
756 Jennings W, Kozak KH, McPeck MA, Moreno-Roark F, Near TJ, et al. 2010.  
757 Early bursts of body size and shape evolution are rare in comparative data.  
758 *Evolution* (N. Y). 64:2385–2396.

759 Hird SM. 2019. Microbiomes, community ecology, and the comparative method.  
760 *mSystems* 4:1–5.

761 Hird SM, Sánchez C, Carstens BC, Brumfield RT. 2015. Comparative Gut Microbiota  
762 of 59 Neotropical Bird Species. *Front. Microbiol.* 6:1403.

763 Jetz W, Thomas GH, Joy JB, Hartmann K, Mooers AO. 2012. The global diversity of  
764 birds in space and time. *Nature* 491:444–448.

765 Knight R, Vrbanac A, Taylor BC, Aksenov A, Callewaert C, Debelius J, Gonzalez A,  
766 Kosciolk T, McCall LI, McDonald D, et al. 2018. Best practices for analysing  
767 microbiomes. *Nat. Rev. Microbiol.* 16:410–422.

768 Kohl KD. 2020. Ecological and evolutionary mechanisms underlying patterns of  
769 phyllosymbiosis in host-associated microbial communities. *Philos. Trans. R. Soc.*  
770 *B Biol. Sci.* 375:20190251.

771 Kohl KD, Dearing MD, Bordenstein SR. 2018. Microbial communities exhibit host  
772 species distinguishability and phyllosymbiosis along the length of the  
773 gastrointestinal tract. *Mol. Ecol.* 27:1874–1883.

774 Labrador M del M, Doña J, Serrano D, Jovani R. 2021. Quantitative interspecific  
775 approach to the stylosphere: Patterns of bacteria and fungi abundance on  
776 passerine bird feathers. *Microb. Ecol.* 81:1088–1097.

777 Lavrinienko A, Jernfors T, Koskimäki JJ, Pirttilä AM, Watts PC. 2021. Does  
778 intraspecific variation in rDNA copy number affect analysis of microbial  
779 communities? *Trends Microbiol.* 29:19–27.

780 Ley RE, Lozupone CA, Hamady M, Knight R, Gordon JI. 2008. Worlds within worlds:  
781 evolution of the vertebrate gut microbiota. *Nat. Rev. Microbiol.* 6:776–788.

782 Lim SJ, Bordenstein SR. 2020. An introduction to phyllosymbiosis. *Proc. R. Soc. B*  
783 *Biol. Sci.* 287:20192900.

784 Martins EP, Hansen TF. 1997. Phylogenies and the comparative method: A general  
785 approach to incorporating phylogenetic information into the analysis of  
786 interspecific data. *Am. Nat.* 149:646–667.

787 Mazel F, Davis KM, Loudon A, Kwong WK, Groussin M, Parfrey LW. 2018. Is host  
788 filtering the main driver of phyllosymbiosis across the Tree of Life? Bik H, editor.  
789 *mSystems* 3:1–15.

790 McFall-Ngai M, Hadfield MG, Bosch TCG, Carey H V., Domazet-Lošo T, Douglas  
791 AE, Dubilier N, Eberl G, Fukami T, Gilbert SF, et al. 2013. Animals in a bacterial  
792 world, a new imperative for the life sciences. *Proc. Natl. Acad. Sci.* 110:3229–  
793 3236.

794 Mirpuri J, Raetz M, Sturge CR, Wilhelm CL, Benson A, Savani RC, Hooper L V,  
795 Yarovinsky F. 2013. Proteobacteria-specific IgA regulates maturation of the  
796 intestinal microbiota. *Gut Microbes* 5:28–39.

797 Moran NA, Ochman H, Hammer TJ. 2019. Evolutionary and ecological  
798 consequences of gut microbial communities. *Annu. Rev. Ecol. Evol. Syst.*  
799 50:451–475.

800 Nishida AH, Ochman H. 2018. Rates of gut microbiome divergence in mammals.  
801 *Mol. Ecol.* 27:1884–1897.

802 Ochman H, Worobey M, Kuo CH, Ndjanga JBN, Peeters M, Hahn BH, Hugenholtz P.  
803 2010. Evolutionary relationships of wild hominids recapitulated by gut microbial  
804 communities. *PLoS Biol.* 8:3–10.

805 Oksanen J, Kindt R, Pierre L, O’Hara B, Simpson GL, Solymos P, Stevens MH. HH,  
806 Wagner H, Blanchet FG, Kindt R, et al. 2016. *vegan: Community Ecology*  
807 *Package, R package version 2.4-0. R Packag. version 2.2-1.*

808 Pagel M. 1999. Inferring the historical patterns of biological evolution. *Nature*  
809 401:877–884.

810 Perez-Lamarque B, Krehenwinkel H, Gillespie RG, Morlon H. 2022. Limited evidence  
811 for microbial transmission in the phyllosymbiosis between Hawaiian spiders and  
812 their microbiota. Hird SM, editor. *mSystems* 7:e01104-21.

813 Perez-Lamarque B, Maliet O, Pichon B, Selosse M-A, Martos F, Morlon H. 2022. Do  
814 closely related species interact with similar partners? Testing for phylogenetic  
815 signal in bipartite interaction networks. *Peer Community J.* 2:e59.

816 Perez-Lamarque B, Morlon H. 2019. Characterizing symbiont inheritance during  
817 host–microbiota evolution: Application to the great apes gut microbiota. *Mol.*  
818 *Ecol. Resour.* 19:1659–1671.

819 Perez-Lamarque B, Morlon H. 2022. Comparing different computational approaches  
820 for detecting long-term vertical transmission in host-associated microbiota. *Mol.*  
821 *Ecol.*

822 Pigliucci M. 2003. Phenotypic integration: Studying the ecology and evolution of  
823 complex phenotypes. *Ecol. Lett.* 6:265–272.

824 Quince C, Curtis TP, Sloan WT. 2008. The rational exploration of microbial diversity.  
825 *ISME J.* 2:997–1006.

826 R Core Team. 2022. *R: A language and environment for statistical computing.*

827 Revell LJ. 2012. *phytools: An R package for phylogenetic comparative biology (and*  
828 *other things).* *Methods Ecol. Evol.* 3:217–223.

829 Revell LJ, Harmon LJ, Collar DC. 2008. Phylogenetic signal, evolutionary process,  
830 and rate. *Syst. Biol.* 57:591–601.

831 Sanders JG, Powell S, Kronauer DJC, Vasconcelos HL, Frederickson ME, Pierce

832 NE. 2014. Stability and phylogenetic correlation in gut microbiota: lessons from  
833 ants and apes. *Mol. Ecol.* 23:1268–1283.

834 Shealy NG, Yoo W, Byndloss MX. 2021. Colonization resistance: metabolic warfare  
835 as a strategy against pathogenic Enterobacteriaceae. *Curr. Opin. Microbiol.*  
836 64:82–90.

837 Shin NR, Whon TW, Bae JW. 2015. Proteobacteria: Microbial signature of dysbiosis  
838 in gut microbiota. *Trends Biotechnol.* 33:496–503.

839 Song SJ, Sanders JG, Delsuc F, Metcalf J, Amato K, Taylor MW, Mazel F, Lutz HL,  
840 Winker K, Graves GR, et al. 2020. Comparative analyses of vertebrate gut  
841 microbiomes reveal convergence between birds and bats. *MBio* 11:1–14.

842 Stan Development Team. 2022. RStan: the R interface to Stan.

843 Thompson LR, Sanders JG, McDonald D, Amir A, Ladau J, Locey KJ, Prill RJ,  
844 Tripathi A, Gibbons SM, Ackermann G, et al. 2017. A communal catalogue  
845 reveals Earth’s multiscale microbial diversity. *Nature* 551:457–463.

846 Trevelline BK, Sosa J, Hartup BK, Kohl KD. 2020. A bird’s-eye view of  
847 phyllosymbiosis: weak signatures of phyllosymbiosis among all 15 species of  
848 cranes. *Proc. R. Soc. B Biol. Sci.* 287:20192988.

849 Upham NS, Esselstyn JA, Jetz W. 2019. Inferring the mammal tree: Species-level  
850 sets of phylogenies for questions in ecology, evolution, and  
851 conservation. Tanentzap AJ, editor. *PLoS Biol.* 17:e3000494.

852 Uyeda JC, Caetano DS, Pennell MW. 2015. Comparative analysis of principal  
853 components can be misleading. *Syst. Biol.* 64:677–689.

854 Wagner MR, Lundberg DS, Del Rio TG, Tringe SG, Dangl JL, Mitchell-Olds T. 2016.  
855 Host genotype and age shape the leaf and root microbiomes of a wild perennial  
856 plant. *Nat. Commun.* 7:12151.

857 Wilman H, Belmaker J, Simpson J, de la Rosa C, Rivadeneira MM, Jetz W. 2014.  
858 EltonTraits 1.0: Species-level foraging attributes of the world’s birds and  
859 mammals. *Ecology* 95:2027–2027.

860